Exome scale liquid biopsy characterization of putative neoantigens and genomic biomarkers pre- and post anti-PD-1 therapy in squamous cell carcinoma of the head and neck

Charles W. Abbott[1], Nikita Bedi[2], Simo V. Zhang[1], Mengyao Tan[1],Robin Li[1], Rachel Marty Pyke[1], Eric Levy[1], Rebecca Chernock[3], Mena Mansour[3], John B. Sunwoo[2], A. Dimitrios Colevas[2], Sean M. Boyle[1], Richard Chen[1]
[1]Personalis, Inc., Menlo Park, CA; [2]Stanford University, Stanford, CA; [3]Washington University in St. Louis, St. Louis, MO.
charles.abbott@personalis.com

Background

The reduced scope, and number of genes profiled by typical liquid biopsy panels can result in missed biomarkers including neoantigens, which may change with treatment, as well as potentially undetected resistance mechanisms and pathways beyond the scope of targets typically captured by panels. To address these limitations, we used a whole-exome scale liquid biopsy monitoring platform, NeXT Liquid Biopsy, to analyze head and neck squamous cell carcinoma (HNSCC) patients that have received anti-PD1 therapy. Presently, we sought to (1) monitor neoantigen changes in cfDNA as a complement to tumor biopsy-derived neoantigens, (2) compare the impact of tumor escape mechanisms, including HLA-LOH, on neoantigens identified in tissue and cfDNA and (3) to identify novel biological signatures that combine information from both solid tumor and liquid biopsies.

Methods

Pre- and post-intervention matched tumor, normal and plasma samples were obtained from a pilot cohort of 9 patients with HNSCC. Following initial sample collection all patients received a single dose of nivolumab, followed by definitive resection of the primary tumor mass approximately one month later when possible, or a second biopsy where resection was impractical (resection, n=5; biopsy, n=4). Solid tumor and matched normal samples were profiled using ImmunoID NeXT, an augmented exome/transcriptome platform and analysis pipeline which produces comprehensive tumor mutation information, gene expression quantification, neoantigen characterization, HLA typing and LOH, TCR repertoire profiling and tumor microenvironment data. For the plasma samples, we performed exome-scale cfDNA profiling with the ImmunoID NeXT Liquid Biopsy platform to detect somatic variants. Data from these two platforms were compared with corresponding clinical findings.

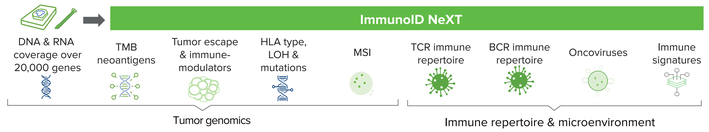

Results

Patient demographics

n	Responder (3)	Non-responder (4)	P-value
Age at treatment	57±7.62)	67.5±3.70	0.22
Disease origin			1
Hard palate	1(20%)	0(0%)	1
Left alveolar ridge	0(0%)	1(25%)	1
Left lateral tongue	1(20%)	1(25%)	1
Retromolar trigone	0(0%)	1(25%)	1
Right glabellar (skin)	1(20%)	0(0%)	1
Right lateral tongue	1(20%)	0(0%)	1
Scalp and neck (skin)	1(20%)	1(25%)	1
Intervention			0.52
Nivolumab	1(20%)	2(50%)	0.81
Nivolumab (in combination with resection)	4(80%)	2(50%)	0.81
Sex			1
Female	3(60%)	2(50%)	1
Male	2(40%)	2(50%)	1
Stage at treatment			0.52
III	4(80%)	2(50%)	0.81
IV	1(20%)	2(50%)	0.81

The demographics of the two groups of HNSCC subjects were similar. Baseline characteristics were summarized for each treatment group and presented as frequency distributions and/or summary statistics. Baseline data for all comparisons were those values recorded before immunotherapy, at the time of initial biopsy. Patient responses, as defined by standard RECIST criteria, or histological assessment were classified as either responder or non-responder. One patient stopped early due to biopsy proven metastatic disease. A second patient with early reccurrence and metastatic disease received subsequent chemoradiation (Cisplatin and 66Gy).

Concordant somatic events in tumor and plasma

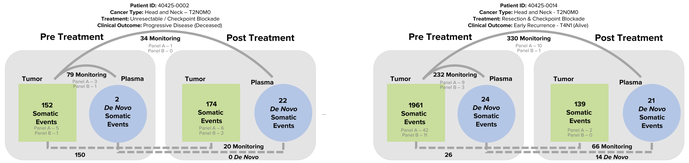

Noninvasive detection of disease, and monitoring of therapeutic response via liquid biopsy of cfDNA is a growing area of cancer research with considerable implications for clinical management. Liquid biopsy is particularly attractive in cases where multiple biopsies are needed for longitudinal monitoring of disease progression. Above, we explore the concordance observed between somatic events observed in solid tumor, and those detected in plasma in a pre/post therapeutic intervention paradigm. To establish concordance, we tracked the mutational status in matched tumor/plasma cases. Strong concordance was observed in all patients, with a large number of somatic events occuring in genes not traditionally covered in clinical NGS panels.

Mutational landscape of circulating tumor DNA

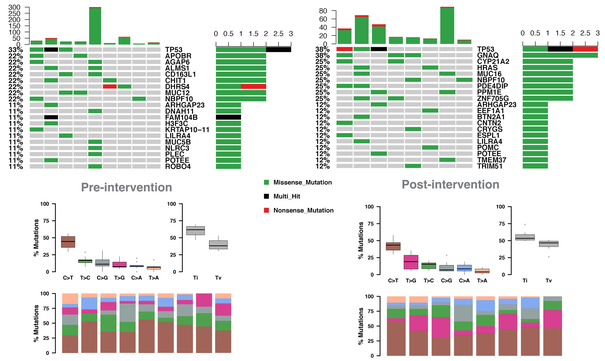

The mutational landscape of circulating cfDNA in patients pre- and post-intervention was investigated. The most commonly identified mutation occurred in TP53, which was identified in 3 patients at both treatment timepoints. GNAQ, which is involved in GTPase activity, was initially found in a single subject pre-intervention, and in two additional patients post-intervention. Appearance of new mutations in this manner could be due, at least in part, to increased tumor shedding in response to therapy.

C>T transitions made up the bulk of identified SNVs, and remained consistent through treatment (~45%, across both timepoints). We observed a marked increase in T>G transversions which expanded from ~7% pre-intervention to ~19% post-intervention.

Dynamic VAF in response to intervention

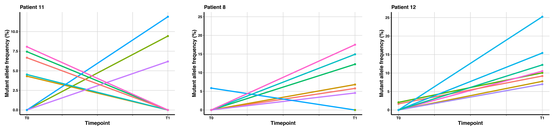

Large shifts in variant allele frequency (VAF) were detected in all patients despite the relatively short period of time between pre- and post-intervention timepoints. Genes with the largest absolute VAF changes are highlighted for three patients at left. Patient 11, a responder, shows a greater number of genes with declining VAF than non-responding patients 8 and 12, who present with predominantly increasing VAFs. Further investigation of specific genes that undergo large VAF changes in response to therapy is ongoing, and may help identify additional response and resistance related mutations.

HLA loss of heterozygosity

HLA-LOH and damaging APM mutations reduce capacity for antigen presentation, and may facilitate immune evasion. HLA LOH is increasingly recognized as a major tumor escape mechanism, particularly in immunotherapeutic interventions. Using DASH, a proprietary HLA LOH detection platform, we identified HLA-LOH in 33% of study participants. Patient 9, highlighted below, exhibited allele-specific loss in HLA- A, B and C, likely resulting in a reduced capacity for antigen presentation in that patient.

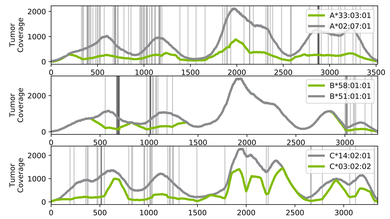

Neoantigen detection in solid and liquid biopsies

Composite neoantigen presentation score (NEOPS), which accounts for impairment to neoantigen presentation and other established resistance markers, was calculated for both solid tumor and cfDNA. In patients 2 (non-responder, blue) and 14 (responder, orange), we observed decrease in neoantigen burden following therapy. Interestingly, these patients presented opposing outcomes in cfDNA, possibly reflecting their differing response to therapy. Tracking NEOPS from both cfDNA and solid tumor may result in a more robust biomarker.

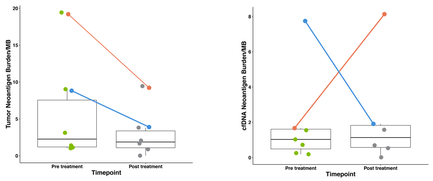

Tumor immune infiltration and immunoregulatory influence

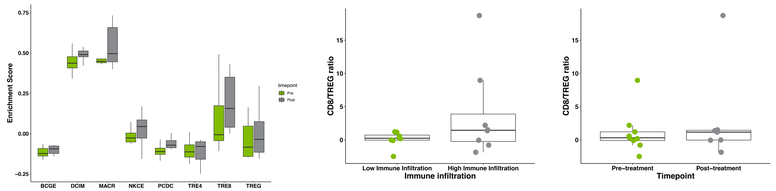

Immune landscape of the tumor microenvironment in HNSCC. TIL enrichment scores for individual cell types are shown. Pre- vs. post-treatment comparisons of 8 different TILs (BCGE, B cell; DCIM, immature dendritic cell; MACR, macrophage; NKCE, natural killer cell; PCDC, plasmacytoid dendritic cell; TRE4, CD4+ T cell; TRE8, CD8+ T cell; TREG, regulatory T cell). CD8/TREG ratios are shown comparing low vs. high immune infiltrated malignancies, and pre vs post treatment.

We investigated TIL infiltration as it is a favorable prognostic factor in a number of cancer types - TILs are associated with increased levels of tumor neoplastic antigens, which may influence response to therapy and overall survival. Additionally, an increased number of TILs has been associated with response and favorable prognosis in most clinical trials evaluating the efficacy of PD-1/PD-L1 inhibitors. To evaluate TILs in both HPV+ and HPV– HNSCC tumors, we generated gene expression profiles from purified immune cells representing different cell lineages. These profiles were then used to create immune cell specific reference gene signatures, enabling quantification of cellular abundances. Using ssGSEA we found consistent enrichment of all cell types following therapeutic intervention, suggesting at least some level of immune response to therapy, irrespective of patient outcome.

Leveraging the TILs data, we investigated the CD8+/Treg cell ratio, and found that it trended higher in the immune-high population compared with the immune-low population, with notable increases at the subject level, suggesting that despite higher overall immune infiltration in the immune-high population, immune-high tumors experience reduced immunoregulatory influence. When stratifying HNSCC tumors by treatment timepoint, we observed small subject-level variances. Prior to treatment, tumors display generally lower levels of T cell infiltration, but consistent immunoregulatory influence as represented by their comparatively similar CD8+/Treg ratio. In agreement with these findings, we also detected a trend of increased cytolytic activity, as captured by the cytolytic activity score (CYT).

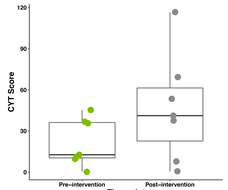

Transcriptomic analysis

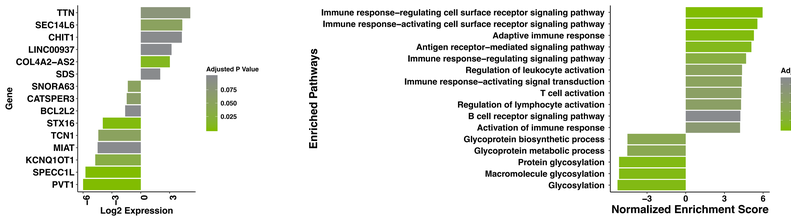

We next investigated transcriptomic profiles within the cohort. Shown here are the top 15 genes differentially expressed in post- versus pre-treatment. Pathway analyses were conducted using PAGE (Parametric Analysis of Gene Set Enrichment) to identify pathway level changes associated with therapeutic intervention. Notably, post-treatment patients were significantly enriched relative to pre-treatment, for pathways involved in immune response including antigen receptor mediated signaling, T cell activation and regulation of lymphocyte activation.

Conclusions

Concordant somatic events were detected between plasma and tumor at pre- and post-treatment timepoints. Neoantigens predicted to arise from these somatic events were reduced in solid tumor post-treatment, but increased in cfDNA, when compared to pre-treatment timepoints. HLA LOH was identified in a number of subjects, likely resulting in reduced neoepitope presentation in those cases. Immune cell infiltration increased in the tumor following treatment, with no changes to the CD8+/Treg cell ratio, suggesting consistent immunoregulation.